Supporting Information

Lupardus et al. 10.1073/pnas.1401180111

SI Methods

TYK2 Expression and Purification for Crystallization. Human TYK2 comprised of residues 566–1187 and containing a kinase-inactivating mutation (D1023N) was cloned into a pAC-based baculovirus expression vector in frame with an N-terminal 6×His and TEV protease tag (MSYYHHHHHHDYDIPTTENLYFQ). After viral recombination and amplification according to standard techniques (Baculogold System; BD Biosciences), 10 L of *Trichoplusia ni* cells were grown in a WAVE (GE Biosciences) bioreactor to 2×10^6 cells per mL and infected with TYK2-containing baculovirus at a multiplicity of infection of 2. The cells were harvested at 48 h postinfection by centrifugation and frozen at −80 °C. Frozen cells from 2 L of cell paste were thawed in extraction buffer [20 mM imidazole, pH 7.0, 250 mM NaCl, 5 mM 2-mercaptoethanol, and 10% (vol/vol) glycerol] plus 0.05% Brij 35. Cells were homogenized and passed once through a Microfluidizer. The lysate was clarified by ultracentrifugation at 40,000 × *g* for 1 h. The supernatant was passed through a 0.8-μm filter and loaded onto a 5-mL HiTrap Ni FastFlow column at 4 °C. The column was washed using extraction buffer and then batch eluted using extraction buffer plus 0.3 M imidazole. The protein was loaded directly on to a Superdex 75 (16/60) column equilibrated in 50 mM Bicine, pH 8.5, 250 mM NaCl, 0.5 mM tris(2-carboxyethyl) phosphine (TCEP), and 10% (vol/vol) glycerol. The N-terminal 6×His-TEV tag was left on the protein. Monomeric fractions were pooled, diluted 1:10, and passed through a SP Fast flow resin. The flow through was collected and brought to 0.25 M NaCl by addition of 5 M NaCl. Typical purification yields of TYK2 using this method were in the range of 3–5 mg/L *T. ni* culture. Protein was concentrated to 10 mg/mL and compound 7012 (100 mM in DMSO) added to a final concentration of 1 mM.

Crystallization, Data Collection, and Structure Determination. High-throughput crystallization trials were performed using the Phoenix Robot (Art Robbins) and prepackaged screens by Hampton Research and Qiagen. Sitting drops using 0.2 μL of protein plus 0.2 μL of reservoir were set up at both 4 and 18 °C. Long rods grew at 18 °C after several days. Conditions were optimized to 15% (wt/vol) PEG monomethyl ether 2000, 0.1 M Hepes, pH 7.4, and 1 mM TCEP. Importantly, we found that both the N-terminal 6×His-TEV tag as well as compound 7012 were essential for efficient crystallization of TYK2. We found the N-terminal tag to be essential for crystal formation, despite our finding that these residues remain disordered in our crystal structure. Importantly, analysis of crystal packing indicates that there is room for these disordered amino acids in the crystal lattice. Compound 7012 was also necessary and the only ATP-competitive small-molecule inhibitor to give large, well-diffracting crystals. Incubation with other TYK2-specific compounds gave either no crystals or small, feathery needles unsuitable for diffraction experiments.

Crystals were preserved for data collection by sudden immersion in liquid nitrogen using crystallization reservoir augmented with 20% (vol/vol) ethylene glycol. A total of six datasets was collected at 110 K at Stanford Synchrotron Radiation Lightsource and Advanced Light Source (ALS) and processed according to space group I4, most of which revealed significant twinning. Final refinement was performed using a 2.8-Å dataset from an ALS beamline 5.0.1 (collected at 0.979 Å), which was reported by phenix.xtriage as not twinned (Table S1). The structure was solved by molecular replacement (Phaser) using the coordinates of the TYK2 kinase domain complexed with compound 7012 as the search probe applied to a 3-Å dataset from ALS 5.0.2. Inferior *Z* values from Phaser suggested which of two copies should be tentatively assigned as the pseudokinase domain. Large and small adjustments to the initial model using Coot, truncation of the pseudokinase domain to a polyalanine model, map inspection using a homology model of the pseudokinase, rigid-body and some restrained refinement using Refmac5 and phenix.refine led to a 3,818-atom model with R_{free} = 36% at 3-Å resolution. Remaining refinements were performed using the nominally untwinned 2.8-Å dataset, but while refining a twin fraction that converged to about 0.06. Manual building, application of the phenix.autobuild wizard, simulated annealing refinement in phenix.refine, and translation/libration/screw refinements led to the final 4,385-atom model with R_{free} = 25.7%. Ramachandran analysis indicates that 92% of the residues lie in the favored position, with 2.3% outliers. The final model includes residues Leu579–Gln1177 (UniProt TYK2_HUMAN with Ser1016) except for missing residues Glu611–Glu635, Gly787–Ser790, Asp872–Asp888, Lys933–Gln939, and Arg1035–Leu1036. The peptide segment between the pseudokinase and kinase domains is incomplete.

TYK2 Purification for Kinase Activity Assays. TYK2 pseudokinase–kinase constructs containing wild-type TYK2 (residues 566–1187) with the described mutations (V768F, R744G, R901S, and delQ586-K587) or TYK2 kinase domain alone (residues 885–1176) were cloned into a pAC-based baculovirus vector in frame with an N-terminal 6×His and TEV protease tag (MSYYHHHHHHDYDIPTTENLYFQ). Viruses were prepared, *T. ni* cells infected, and protein purified as described for crystallization. To obtain an unphosphorylated fraction of the TYK2 mutants for assay and proteolytic digest, size-exclusion chromatography-purified TYK2 mutants were subjected to anion exchange purification on a Mono Q 10/100 GL column (GE Healthcare). Protein was first diluted to 50 mM NaCl in 10 mM Tris, pH 8, 10% (vol/vol) glycerol, and 1 mM TCEP. Protein was bound to the column and eluted with a 50–500 mM NaCl gradient, and individual peaks were assayed by mass spectrometry to determine the nonphosphorylated fraction. For the delQ586-K587 mutant, only enough protein was obtained from the purification for kinase assays. For the R901S mutant, insufficient protein was obtained from the purification to isolate a nonphosphorylated fraction, so only V678F and R744G were tested.

Mass Spectrometry. Mass spectrometry was performed on an Agilent 6224 TOF LC/MS system coupled to an Infinity 1260 HPLC. Proteins were separated on a PLRP-S reversed-phase column using a water/acetonitrile gradient with 0.05% trifluoroacetic acid as counter ion. Mass spectrometry data were analyzed with the MassHunter software (Agilent).

Kinase Assays. The kinase activity of the TYK2 proteins was measured by monitoring phosphorylation of a synthetic peptide derived from the JAK3 protein sequence, 5-FAM-Val-Ala-Leu-Val-Asp-Gly-Tyr-Phe-Arg-Leu-Thr-Thr-NH_2. The peptide is labeled on the N terminus with 5-carboxyfluorescein (5-FAM) and contains a tyrosine residue that can be phosphorylated by TYK2. Due to the wide range of activity of the TYK2 constructs, each sample was serially diluted and tested at multiple concentrations. Reactions (50 μL) contained 100 mM Hepes buffer (pH 7.2), 0.015% Brij 35, 1.5 μM peptide substrate, 25 μM ATP, 10 mM $MgCl_2$, 4 mM DTT, and 0.39–50 nM TYK2 protein. The reactions were incubated at 22 °C in 384-well polypropylene

microtiter plates for 30 min before they were stopped by the addition of 25 μL of 100 mM Hepes buffer (pH 7.2) containing 0.015% Brij 35 and 150 mM EDTA. The peptide substrate in each quenched reaction was electrophoretically separated from phosphorylated product using a LabChip 3000 microfluidic mobility shift instrument (PerkinElmer). The 5-FAM group present on both the substrate and product was excited at 488 nm; the fluorescence at 530 nm was detected and peak heights were reported. The extent (or percentage) of conversion of substrate to product was calculated from the corresponding peak heights in the electropherogram using HTS Well Analyzer, version 5.2, software (PerkinElmer) and the following equation:

$$\%\ \text{conversion} = \{P \div (S + P)\} \times 100,$$

where S and P represent the peak heights of the substrate and product, respectively. The specific activity of each TYK2 protein (i.e., nanomolar concentration of phosphorylated product formed per minute per nanomolar concentration of TYK2) was calculated based on the percentage conversion and the concentration of TYK2 used. The specific activity data (mean ± SD) were taken from the linear regions of plots of percentage conversion vs. enzyme concentration. A total of 5–88 replicate specific activity values was averaged for the various TYK2 constructs.

1. Xiang Z, et al. (2008) Identification of somatic JAK1 mutations in patients with acute myeloid leukemia. *Blood* 111(9):4809–4812.
2. Flex E, et al. (2008) Somatically acquired JAK1 mutations in adult acute lymphoblastic leukemia. *J Exp Med* 205(4):751–758.
3. Asnafi V, et al. (2010) JAK1 mutations are not frequent events in adult T-ALL: A GRAALL study. *Br J Haematol* 148(1):178–179.
4. Tomasson MH, et al. (2008) Somatic mutations and germline sequence variants in the expressed tyrosine kinase genes of patients with de novo acute myeloid leukemia. *Blood* 111(9):4797–4808.
5. Blink M, et al. (2011) Frequency and prognostic implications of JAK 1-3 aberrations in Down syndrome acute lymphoblastic and myeloid leukemia. *Leukemia* 25(8): 1365–1368.
6. Mullighan CG, et al. (2009) JAK mutations in high-risk childhood acute lymphoblastic leukemia. *Proc Natl Acad Sci USA* 106(23):9414–9418.
7. Jeong EG, et al. (2008) Somatic mutations of JAK1 and JAK3 in acute leukemias and solid cancers. *Clin Cancer Res* 14(12):3716–3721.
8. Staerk J, Kallin A, Demoulin JB, Vainchenker W, Constantinescu SN (2005) JAK1 and Tyk2 activation by the homologous polycythemia vera JAK2 V617F mutation: Cross-talk with IGF1 receptor. *J Biol Chem* 280(51):41893–41899.
9. Levine RL, et al. (2005) Activating mutation in the tyrosine kinase JAK2 in polycythemia vera, essential thrombocythemia, and myeloid metaplasia with myelofibrosis. *Cancer Cell* 7(4):387–397.
10. Hama A, et al. (2012) Molecular lesions in childhood and adult acute megakaryoblastic leukaemia. *Br J Haematol* 156(3):316–325.
11. Scott LM (2011) The JAK2 exon 12 mutations: A comprehensive review. *Am J Hematol* 86(8):668–676.
12. Passamonti F, et al. (2011) Molecular and clinical features of the myeloproliferative neoplasm associated with JAK2 exon 12 mutations. *Blood* 117(10):2813–2816.
13. Martínez-Avilés L, et al. (2007) JAK2 exon 12 mutations in polycythemia vera or idiopathic erythrocytosis. *Haematologica* 92(12):1717–1718.
14. Scott LM, et al. (2007) JAK2 exon 12 mutations in polycythemia vera and idiopathic erythrocytosis. *N Engl J Med* 356(5):459–468.
15. Percy MJ, et al. (2007) The frequency of JAK2 exon 12 mutations in idiopathic erythrocytosis patients with low serum erythropoietin levels. *Haematologica* 92(12): 1607–1614.
16. Williams DM, Kim AH, Rogers O, Spivak JL, Moliterno AR (2007) Phenotypic variations and new mutations in JAK2 V617F-negative polycythemia vera, erythrocytosis, and idiopathic myelofibrosis. *Exp Hematol* 35(11):1641–1646.
17. Siemiatkowska A, Bieniaszewska M, Hellmann A, Limon J (2010) JAK2 and MPL gene mutations in V617F-negative myeloproliferative neoplasms. *Leuk Res* 34(3):387–389.
18. Pardanani A, Lasho TL, Finke C, Hanson CA, Tefferi A (2007) Prevalence and clinicopathologic correlates of JAK2 exon 12 mutations in JAK2V617F-negative polycythemia vera. *Leukemia* 21(9):1960–1963.
19. Butcher CM, et al. (2008) Two novel JAK2 exon 12 mutations in JAK2V617F-negative polycythaemia vera patients. *Leukemia* 22(4):870–873.
20. Colaizzo D, et al. (2007) A new JAK2 gene mutation in patients with polycythemia vera and splanchnic vein thrombosis. *Blood* 110(7):2768–2769.
21. Pietra D, et al. (2008) Somatic mutations of JAK2 exon 12 in patients with JAK2 (V617F)-negative myeloproliferative disorders. *Blood* 111(3):1686–1689.
22. Kratz CP, et al. (2006) Mutational screen reveals a novel JAK2 mutation, L611S, in a child with acute lymphoblastic leukemia. *Leukemia* 20(2):381–383.
23. Funakoshi-Tago M, Pelletier S, Moritake H, Parganas E, Ihle JN (2008) Jak2 FERM domain interaction with the erythropoietin receptor regulates Jak2 kinase activity. *Mol Cell Biol* 28(5):1792–1801.
24. James C, et al. (2005) A unique clonal JAK2 mutation leading to constitutive signalling causes polycythaemia vera. *Nature* 434(7037):1144–1148.
25. Zhao R, et al. (2005) Identification of an acquired JAK2 mutation in polycythemia vera. *J Biol Chem* 280(24):22788–22792.
26. Baxter EJ, et al.; Cancer Genome Project (2005) Acquired mutation of the tyrosine kinase JAK2 in human myeloproliferative disorders. *Lancet* 365(9464):1054–1061.
27. Kralovics R, et al. (2005) A gain-of-function mutation of JAK2 in myeloproliferative disorders. *N Engl J Med* 352(17):1779–1790.
28. Schnittger S, et al. (2006) Report on two novel nucleotide exchanges in the JAK2 pseudokinase domain: D620E and E627E. *Leukemia* 20(12):2195–2197.
29. Bercovich D, et al. (2008) Mutations of JAK2 in acute lymphoblastic leukaemias associated with Down's syndrome. *Lancet* 372(9648):1484–1492.
30. Kearney L, et al. (2009) Specific JAK2 mutation (JAK2R683) and multiple gene deletions in Down syndrome acute lymphoblastic leukemia. *Blood* 113(3):646–648.
31. Gaikwad A, et al. (2009) Prevalence and clinical correlates of JAK2 mutations in Down syndrome acute lymphoblastic leukaemia. *Br J Haematol* 144(6):930–932.
32. Malinge S, et al. (2007) Novel activating JAK2 mutation in a patient with Down syndrome and B-cell precursor acute lymphoblastic leukemia. *Blood* 109(5): 2202–2204.
33. Mercher T, et al. (2006) JAK2T875N is a novel activating mutation that results in myeloproliferative disease with features of megakaryoblastic leukemia in a murine bone marrow transplantation model. *Blood* 108(8):2770–2779.
34. Kiyoi H, Yamaji S, Kojima S, Naoe T (2007) JAK3 mutations occur in acute megakaryoblastic leukemia both in Down syndrome children and non-Down syndrome adults. *Leukemia* 21(3):574–576.
35. Walters DK, et al. (2006) Activating alleles of JAK3 in acute megakaryoblastic leukemia. *Cancer Cell* 10(1):65–75.
36. Sato T, et al. (2008) Functional analysis of JAK3 mutations in transient myeloproliferative disorder and acute megakaryoblastic leukaemia accompanying Down syndrome. *Br J Haematol* 141(5):681–688.
37. Klusmann JH, et al. (2007) Janus kinase mutations in the development of acute megakaryoblastic leukemia in children with and without Down's syndrome. *Leukemia* 21(7):1584–1587.

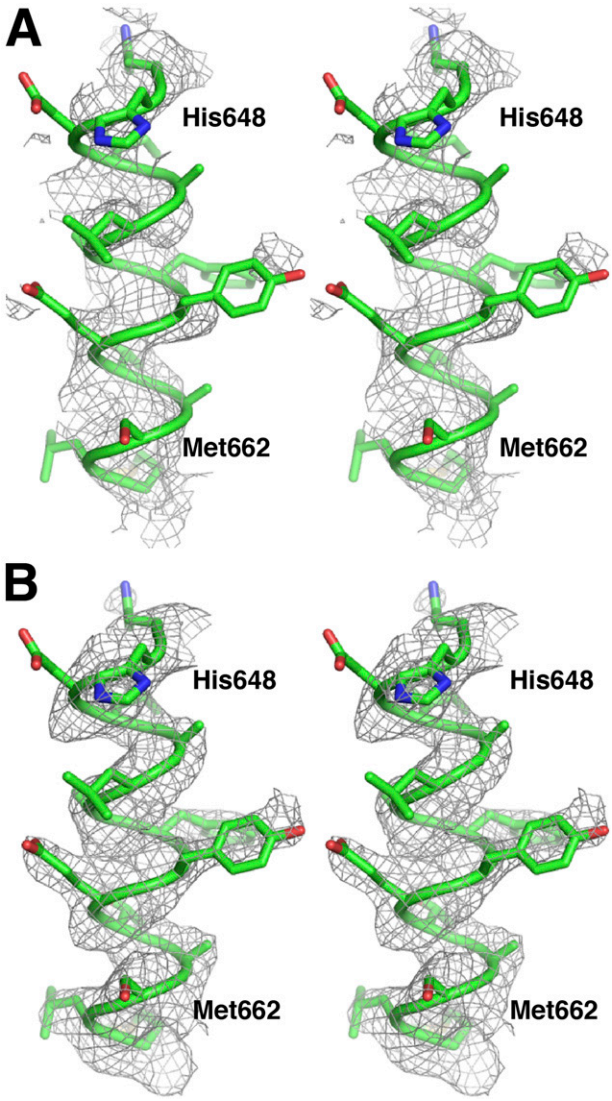

Fig. S1. Electron density maps. Stereo electron density images contoured at 1.0σ shown with final coordinates from the pseudokinase αC-helix. (*A*) Map from molecular replacement using a search probe lacking the entire pseudokinase N-terminal lobe. (*B*) The same region of the final 2mFo-dFc map.

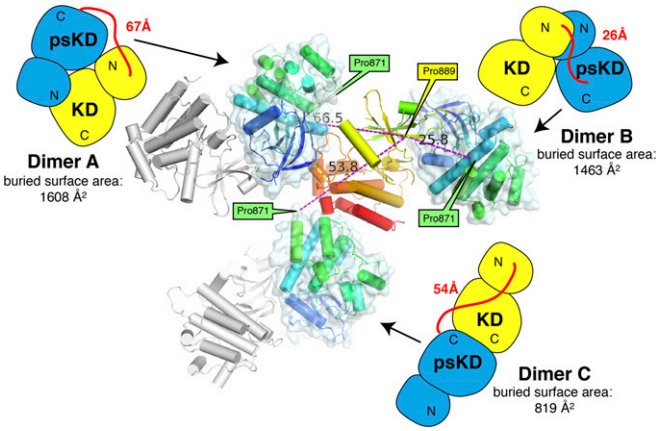

Fig. S2. Identification of the pseudokinase–kinase asymmetric unit. The kinase domain is shown in the center as a cartoon [colored in rainbow from green (N terminus) to red (C terminus)], with three possible pseudokinase domains show as cartoons with surface rendered [colored in rainbow from blue (N terminus) to green (C terminus)]. The linker between the pseudokinase C terminus and kinase N terminus is unstructured, leaving three possible pseudokinase–kinase dimers from analysis of the crystal lattice. Dimer A is arranged head to tail with 67 Å between the C and N termini. Dimer B is arranged back to back, with 26 Å between the termini. Dimer C is arranged end to end, with 54 Å between the termini. Buried surface area for each of these possible dimers is listed in the figure. Two other possible contacts between pseudokinase and kinase subunits that do not touch each other in the lattice had linker distances >60 Å (not shown). Given the constraints of a 17-residue linker (absolute maximum, 3.7 Å per residue), Dimer B is the most reasonable covalently linked configuration.

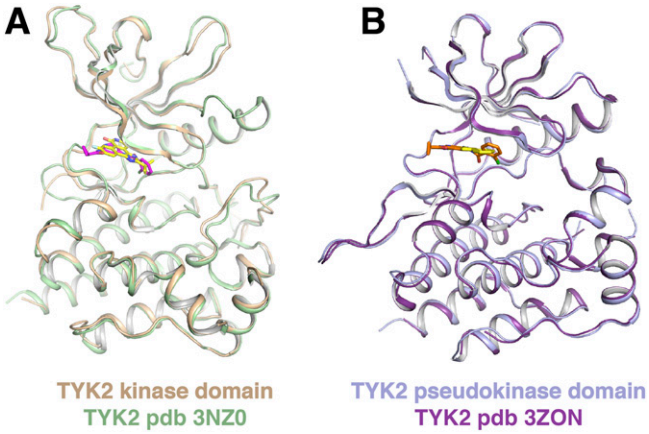

Fig. S3. Comparison of TYK2 pseudokinase–kinase structure to structures of the individual domains. (*A*) Overlay of the TYK2 kinase domain from the pseudokinase–kinase dimer (shown in the color tan with magenta ligand) with the structure of the isolated kinase domain (PDB ID code 3NZ0) (shown in the color green with yellow ligand). (*B*) Overlay of the TYK2 pseudokinase domain from the pseudokinase–kinase dimer (shown in the color blue with orange ligand) with the structure of the isolated pseudokinase domain (PDB ID code 3ZON) (shown in the color purple with yellow ligand). Protein is shown as backbone only with ligands shown as sticks.

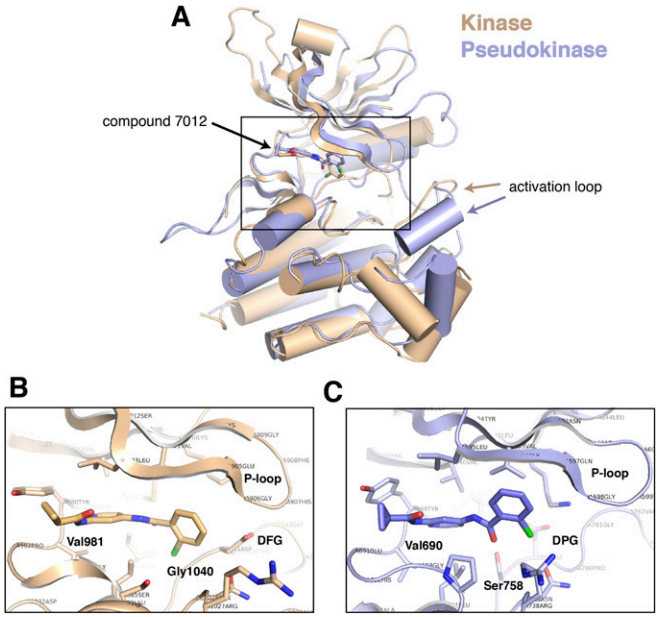

Fig. S4. Comparison of the TYK2 kinase domain to the pseudokinase domain. (*A*) Overlay of the kinase and pseudokinase domains. Protein is shown as a cartoon model, with the kinase shown in tan color, and pseudokinase shown in blue. (*B*) Close-up views of the ligand binding mode for the kinase and (*C*) pseudokinase domains. Colors match those in *A*, and inhibitors (compound 7012) are shown as sticks.

TYK2 KD wild type (aa 885-1176)

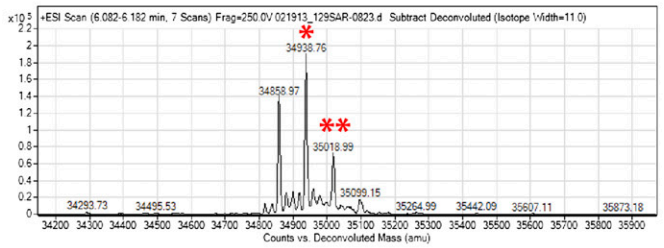

calculated MW = 34948
observed MW = 34858 [-Met (*131Da*), +Acetyl (*42Da*)]
= 34939 [-Met, +Acetyl, +**PO4 (80Da)**]
= 35019 [-Met, +Acetyl, +**2PO4**]

TYK2 psKD/KD R744G

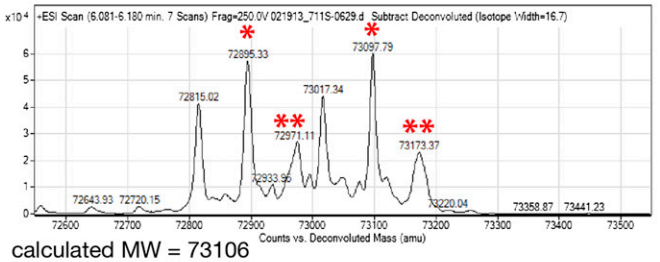

calculated MW = 73106
observed MW = 72815 [-Cterm ValCys, -Met, +Acetyl]
= 72971 [-Cterm ValCys, -Met, +Acetyl, +**PO4**]
= 72971 [-Cterm ValCys, -Met, +Acetyl, +**2PO4**]
= 73017 [-Met, +Acetyl]
= 73097 [-Met, +Acetyl, +**PO4**]
= 73173 [-Met, +Acetyl, +**2PO4**]

TYK2 psKD/KD wild type (aa 566-1187)

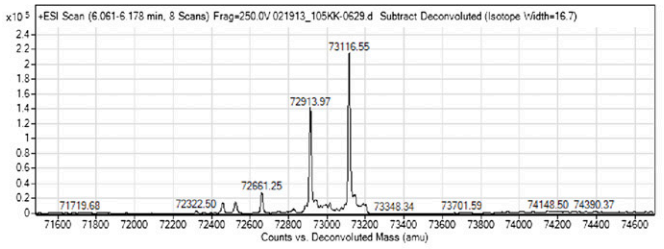

calculated MW = 73205
observed MW = 72913 [-Cterm ValCys (*202Da*) -Met, +Acetyl]
= 73116 [-Met, +Acetyl]

TYK2 psKD/KD R901S

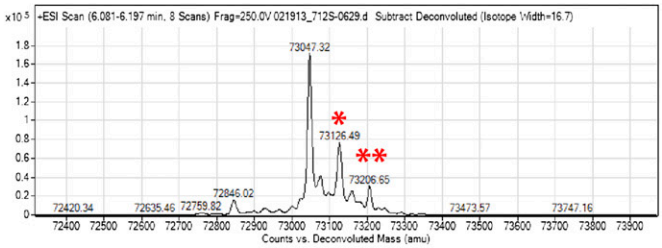

calculated MW = 73136
observed MW = 73047 [-Met, +Acetyl]
= 73126 [-Met, +Acetyl, +**PO4**]
= 73206 [-Met, +Acetyl, +**2PO4**]

TYK2 psKD/KD V678F

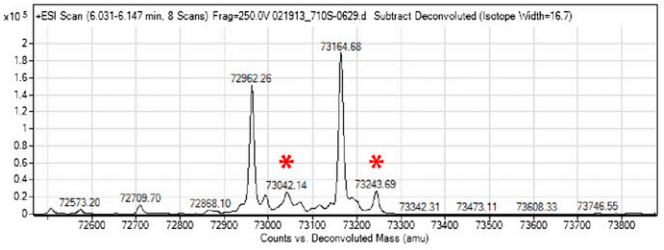

calculated MW = 73253
observed MW = 72962 [-Cterm ValCys, -Met, +Acetyl]
= 73042 [-Cterm ValCys, -Met, +Acetyl, +**PO4**]
= 73165 [-Met, +Acetyl]
= 73244 [-Met, +Acetyl, +**PO4**]

TYK2 psKD/KD delQ586-K587

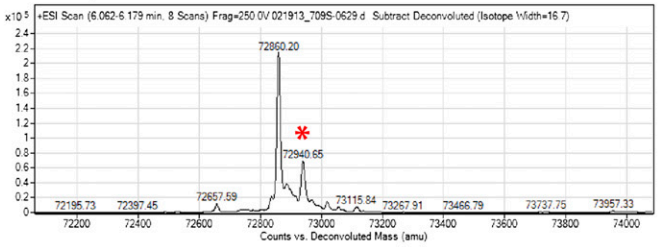

calculated MW = 72949
observed MW = 72860 [-Met, +Acetyl]
= 72940 [-Met, +Acetyl, +**PO4**]

Fig. S5. Mass-spectrometric analysis of TYK2 constructs purified from insect cells. Six TYK2 constructs were analyzed: the wild-type kinase domain (KD, residues 885–1176), the wild-type pseudokinase–kinase domains (psKD/KD, residues 566–1187), and the four pseudokinase–kinase mutants, V678F, R744G, R901S, and delQ586-K587. All major peaks and their modifications are annotated below the mass spectrograms. Peaks corresponding to singly and doubly phosphorylated TYK2 are marked with one or two red asterisks, respectively. All TYK2 constructs had the N-terminal methionine removed and the N terminus acetylated, which removes 89 Da from the mass. Some of the constructs also showed heterogeneity at the C terminus, with the C-terminal valine and cysteine residues absent (minus 202 Da).

TYK2 psKD/KD wild type (aa 566-1187)

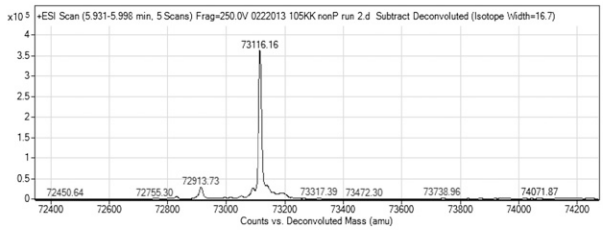

calculated MW = 73205
observed MW = 73116 [-Met, +Acetyl]

TYK2 psKD/KD V678F

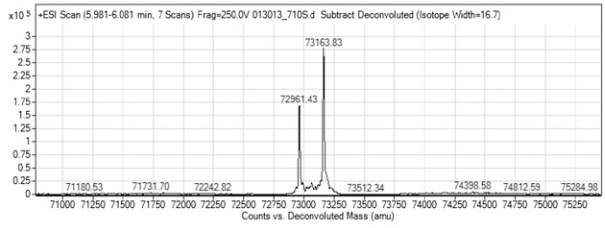

calculated MW = 73253
observed MW = 72961 [-Cterm ValCys, -Met, +Acetyl]
= 73164 [-Met, +Acetyl]

TYK2 psKD/KD R744G

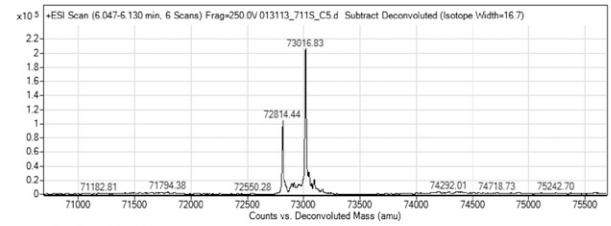

calculated MW = 73106
observed MW = 72814 [-Cterm ValCys, -Met, +Acetyl]
= 73017 [-Met, +Acetyl]

Fig. S6. Mass-spectrometric analysis of nonphosphorylated TYK2 pseudokinase–kinase constructs. Wild-type, V678F, and R744G TYK2 pseudokinase–kinase (psKD/KD) constructs that were purified by Mono Q anion exchange chromatography to isolate nonphosphorylated fractions and mass analyzed. All major peaks and their modifications are annotated below the mass spectrograms. See Fig. S5 legend for details about modifications.

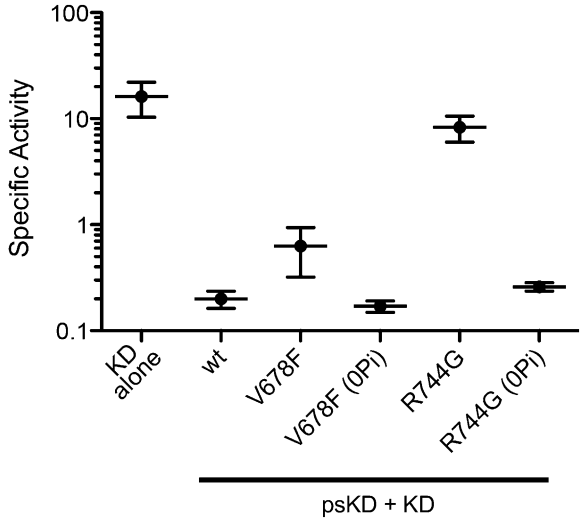

Fig. S7. Nonphosphorylated TYK2 pseudokinase–kinase mutants are inactive in vitro. The activity of the wild-type TYK2 kinase domain (KD, residues 885–1176) was compared with the wild-type TYK2 pseudokinase and kinase domains (wt, residues 566–1187) and the phosphorylated and unphosphorylated forms of two pseudokinase–kinase interface mutants (V678F and R744G). Specific activity was measured in an assay monitoring phosphorylation of a synthetic peptide derived from the JAK3 sequence and calculated based on the percentage conversion to phosphorylated product over time and the concentration of TYK2 used. Values shown have units of nanomolar concentration of product formed per minute per nanomolar concentration of TYK2 and are the mean of more than five measurements ± SD. R901S and delQ586/K587 were not tested due to an inability to purify an unphosphorylated fraction. Values for KD, wt, V678F, and R744G are the same as shown in Fig. 4, but are shown here again for comparison.

Table S1. Data collection and refinement statistics for TYK2 pseudokinase/kinase

	Statistics
Data collection	
Space group	I4
Cell dimensions	
a, *b*, *c*, Å	111.01, 111.01, 123.95
α, β, γ, °	90, 90, 90
Resolution, Å	50–2.8 (2.9–2.8)*
R_{sym}	0.060 (0.587)
$I/\sigma I$	21 (2.2)
Completeness, %	99.5 (99.0)
Redundancy	3.8 (3.7)
Refinement	
Resolution, Å	46.1–2.8
No. reflections	18,446
R_{work}/R_{free}	0.201/0.257
No. atoms	4,396
Protein	4,344
Ligand/ion	44
Water	8
B factors	84
Protein	84
Ligand/ion	64
Water	51
R.m.s. deviations	
Bond lengths, Å	0.010
Bond angles, °	1.2

*Values in parentheses are for highest-resolution shell.

Table S2. Catalog of JAK mutations in cancer

JAK family member	Residues	Location	Cancer type	Constitutive activity?	Ref(s).
Jak1	T478S	SH2	AML	Yes	1
	S512L	SH2	T-ALL		2, 3
	V623A	N-lobe psKD	AML	Yes	1, 4
	D625R	N-lobe psKD	DS-ALL		5
	L624-R629delinsW	N-lobe psKD	Childhood ALL		6
	A634D	N-lobe psKD	B-ALL, T-ALL	Yes	2
	S646F	N-lobe psKD	Childhood ALL	Yes	6
	H647Y	N-lobe psKD	Ductal carcinoma		7
	V651M	N-lobe psKD	DS-ALL		5
	Y652H	N-lobe psKD	T-ALL		3
	L653F	N-lobe psKD	Childhood T-ALL		2
	V658F	N-lobe psKD	Homologous to J2V617F	Yes	6–8
	R724H/Q	N-lobe psKD	T-ALL	Yes	2, 3
	T782M	C-lobe psKD	NSCLC		7
	L783F	C-lobe psKD	T-ALL		7
	R879S/C/H	N-lobe KD	T-ALL	Yes	2
Jak2	R340Q	FERM	PCV		9
	M535I	Exon 12	AMKL		10
	N533IK539L	Exon 12	PCV		11
	F537IK539L	Exon 12	PCV		11
	H538del	Exon 12	PCV		11
	H538-K539del	Exon 12	PCV		11
	H538-K539delinsF	Exon 12	PCV		11
	H538-K539delinsI	Exon 12	PCV		11
	H538-K539delinsL	Exon 12	PCV		11–13
	H538QK539L	Exon 12	PCV		11
	H538DK539LI540S	Exon 12	PCV		11
	K539L	Exon 12	PCV	Yes	11–15
	K539LL545V	Exon 12	PCV		11
	F537-K539del	Exon 12	PCV		11
	F537-K539delinsL	Exon 12	PCV	Yes	11, 12, 14–18
	F537-K539delinsK	Exon 12	PCV		11, 16
	V536F,F537-I546dup10	Exon 12	PCV		11
	V536-I546dup11	Exon 12	PCV		11, 12
	V536-F547dup12	Exon 12	PCV		11, 12
	F537-F547dup11	Exon 12	PCV		11, 12, 17
	H538QK539L	Exon 12	PCV	Yes	11, 12, 14, 16
	I540T	Exon 12	PCV		11
	I540-N542delinsK	Exon 12	PCV		11
	I540-N542delinsS	Exon 12	PCV		11, 12
	I540-E543delinsKK	Exon 12	PCV		11
	I540-E543delinsMK	Exon 12	PCV		11, 12, 19
	I540-D544delinsMK	Exon 12	PCV		11
	I540S,R541-E543delinsK	Exon 12	PCV		11
	R541-E543delinsK	Exon 12	PCV		11, 12, 16, 19, 20
	R541-D544del	Exon 12	PCV		11
	N542-E543del	Exon 12	PCV	Yes	11–15, 18
	N542-D544delinsN	Exon 12	PCV		11
	E543del	Exon 12	PCV		12
	E543-D544del	Exon 12	PCV		11, 12, 15
	D544G	Exon 12	PCV		11
	L545S	Exon 12	PCV		11
	D544-L545del	Exon 12	PCV		11
	F537-I546dupF547L	Exon 12	PCV		11, 12, 21
	F547L, I540-F547dup8	Exon 12	PCV		11, 12
	F547L	Exon 12	PCV		11
	F547V	Exon 12	PCV		11, 12
	R564L	N-lobe psKD	PCV		9
	L611S	N-lobe psKD	Childhood ALL		22
	Y613E	N-lobe psKD	In vitro	Yes	23
	V617F	N-lobe psKD	PCV	Yes	9, 24–27
	D620E	N-lobe psKD	Unclassifiable MPS		28

Table S2. Cont.

JAK family member	Residues	Location	Cancer type	Constitutive activity?	Ref(s).
	I682F	N-lobe psKD	Childhood ALL	Yes	6
	L681-I682insTPYEGMPGH	N-lobe psKD	DS-ALL		29
	I682delinsMPAP	N-lobe psKD	DS-ALL		29
	R683G/S/K/T	N-lobe psKD	Childhood ALL, Downs ALL	Yes	6, 29–31
	QGinsR683	N-lobe psKD	ALL		6
	GPlinsR683	N-lobe psKD	DS-ALL		5
	R683insQG	N-lobe psKD	Childhood ALL		6
	Del682-686	N-lobe psKD	DS-ALL	Yes	32
	Y813D	psKD-KD linker	IMF		17
	R867Q	N-lobe KD	Childhood ALL		6
	D873N	N-lobe KD	Childhood ALL	Yes	6
	T875N	N-lobe KD	AMKL	Yes	33
	P933R	N-lobe KD	Childhood ALL	Yes	6
	R1063H	C-lobe KD	ET/PCV		9, 17
	N1108S	C-lobe KD	PCV		17
Jak3	I87T	FERM	DS TMD		34
	P132T	FERM	Non-DS AMKL	Yes	35
	Q501H	SH2-psKD linker	AMKL		10
	A572V	N-lobe psKD	AMKL	Yes	35, 36
	A573V	N-lobe psKD	DS-ALL,DS AMKL	Yes	5, 32, 34
	M576L	N-lobe psKD	Adult non-DS AMKL		34
	A593T	N-lobe psKD	DS AMKL		34
	R657Q	N-lobe psKD	AML cell line	Yes	36
	V715I	C-lobe psKD	Ductal carcinoma		7
	V722I	C-lobe psKD	AMKL	Yes	32, 34, 35, 37
	S789P	C-lobe psKD	Childhood ALL		6

ALL, acute lymphoblastic leukemia; AMKL, acute megakaryoblastic leukemia; AML, acute myeloid leukemia; DS-ALL, Down syndrome acute lymphoblastic leukemia; DS TMD, Down syndrome transient myeloproliferative disorder; ET/PCV, essential thrombocythemia/polycythemia vera; IMF, idiopathic myelofibrosis; MPS, myeloproliferative syndrome; NSCLC, non–small-cell lung carcinoma; PCV, polycythemia vera; T-ALL, T-cell acute lymphoblastic leukemia.